

A dozen colliding wind X-ray binaries in the star cluster R 136 in the 30 Doradus region

Simon F. Portegies Zwart^{1,2,3}, David Pooley³, Walter, H. G. Lewin³

arXiv:astro-ph/0106109v2 9 Apr 2002

¹Astronomical Institute “Anton Pannekoek”, Univeristy of Amsterdam, Kruislaan 403, 1098 SJ Amsterdam, NL

²Section Computational Science, Univeristy of Amsterdam, Kruislaan 403, 1098 SJ Amsterdam, NL

³Massachusetts Institute of Technology, Cambridge, MA 02139, USA

Subject headings: stars: early-type — stars: Wolf-Rayet — galaxies:) Magellanic Clouds — X-rays: stars — X-rays: binaries — globular clusters: individual (R136)

ABSTRACT

We analyzed archival *Chandra* X-ray observations of the central portion of the 30 Doradus region in the Large Magellanic Cloud. The image contains 20 X-ray point sources with luminosities between 5×10^{32} and 2×10^{35} erg s⁻¹ (0.2 – 3.5 keV). A dozen sources have bright WN Wolf-Rayet or spectral type O stars as optical counterparts. Nine of these are within ~ 3.4 pc of R 136, the central star cluster of NGC 2070. We derive an empirical relation between the X-ray luminosity and the parameters for the stellar wind of the optical counterpart. The relation gives good agreement for known colliding wind binaries in the Milky Way Galaxy and for the identified X-ray sources in NGC 2070. We conclude that probably all identified X-ray sources in NGC 2070 are colliding wind binaries and that they are not associated with compact objects. This conclusion contradicts Wang (1995) who argued, using *ROSAT* data, that two earlier discovered X-ray sources are accreting black-hole binaries. Five of the eighteen brightest stars in R 136 are not visible in our X-ray observations. These stars are either single, have low mass companions or very wide orbits. The resulting binary fraction among early type stars is then unusually high (at least 70%).

1. Introduction

30 Doradus (NGC 2070) is an active star forming region in the Large Magellanic Cloud (LMC). Its most striking feature in the optical is the young and compact star cluster R 136 (HD 38268; see Walborn 1973). The cluster was long thought to be a single star with a mass exceeding $3000 M_{\odot}$ (Cassinelli et al. 1981). The discovery that this “single star” fitted a King (1966) model indicated that the object is in fact a cluster of stars (Weigelt & Baier 1985). Later the *Hubble Space Telescope* provided direct proof for this hypothesis by resolving the cluster into individual stars (Campbell et al. 1992; Massey & Hunter 1998).

The structural parameters of R 136 — mass (21 000 – 79 000 M_{\odot}), half-mass radius (~ 0.5 pc), and density profile ($W_0 \sim 6$, see e.g. Campbell et al. 1992; Brandl et al. 1996; and Massey & Hunter 1998) — are quite similar to three well known counterparts in the Milky Way Galaxy: the Arches cluster (Object 17, Nagata et al. 1995), the Quintuplet (AFGL 2004, Nagata et al. 1990; Okuda et al. 1990), and NGC 3603 (Brandl 1999). All being younger than ~ 3 Myr, these clusters are also comparable in age. NGC 3603 is hidden behind a spiral arm, but is much easier to observe than the Arches and the Quintuplet, which are located near Galactic coordinates $l = 0.122^{\circ}$, $b = 0.018^{\circ}$ (~ 35 pc in projection)

of the Galactic center. The extinction in the direction of the Galactic center easily exceeds 20 magnitudes in visual. R 136 is conveniently located in the LMC and therefore is quite unique as it is neither obscured by dust and gas nor perturbed by external tidal fields; the tidal effect of the LMC is negligible (see Portegies Zwart et al. 1999). The large distance of about 50 kpc, however, limits the observability of the cluster. Note that the star clusters Westerlund 1 and 2 (Westerlund 1960, 1961) both have rather similar characteristics as the above mentioned clusters.

In 1991, Wang & Helfand studied the 30 Doradus region with the *Einstein* Imaging Proportional Counter. They found that hot gas surrounds a ~ 300 pc area around R 136. They also found two marginally significant point sources with the *Einstein* High Resolution Imager in the central area of 30 Doradus. A follow-up with the *ROSAT* High Resolution Imager confirmed the presence of two point sources. Wang (1995) analyzed these two sources and used their similarities with Cyg X-1, LMC X-1 and LMC X-3 to conclude that the observed X-ray sources in 30 Doradus also host black holes. Recent XMM observations by Dennerl et al. (2001) showed a wealth of X-ray sources in the 30 Doradus region. They pay little attention, however, to the X-ray point sources in R 136. In a preliminary study of *Chandra* data of R 136, Feigelson (2000, see also Townsley et al 2001, in preparation) mentions the presence of a dozen bright X-ray sources with O3 or WN star companions. He argues that the dimmer sources could be colliding wind binaries, but that the brighter sources are probably X-ray binaries with neutron star or black hole primaries. From a practical point of view, however, there are some difficulties associated with claims that there are neutron stars or black holes in R 136.

The most massive stars in R 136 exceed $120 M_{\odot}$. Massey & Hunter (1998) took high resolution spectra of the brightest 65 stars and concluded that their age is $< 1\text{--}2$ Myr, where the intermediate mass stars are slightly older 4–5 Myr (Siriani et al. 2000). They also argue that the high abundance of stars with spectral type O3 and earlier is a consequence of the young age of the cluster. de Koter et al. (1997) analyzed the spectra of the most massive stars in R 136 and concluded that the ages of these stars are $\lesssim 1.5$ Myr, which is consistent with the results by Massey & Hunter (1998).

The hydrogen and helium burning age of a $120 M_{\odot}$ star depends quite sensitively on its metallicity Z , being as low as 2.87 Myr for a $Z = 0.001$ (the solar metallicity $Z_{\odot} = 0.02$) to 4.96 Myr for $Z = 0.04$ (Meynet et al. 1994). Because R136 is only ~ 2 Myr old, no star in it can have left the main sequence yet. It would therefore be quite remarkable if the star cluster were able to produce black holes before 2 Myr.

We analyze archival *Chandra* data of the central portion of the 30 Doradus region and confirm the detection of the two X-ray point sources previously found by Wang & Helfand

(1991). In addition, we find 18 new X-ray sources, of which 13 have WN Wolf-Rayet stars or early type O3f* stars as optical counterparts. One of these X-ray sources is probably a blend of several WN stars in the sub-cluster R 140 (to the north of R 136). We argue that the X-rays produced by these systems originate from the colliding winds of the early type stars. The X-ray luminosities of three of these stars are an order of magnitude higher than the X-ray luminosities of colliding wind systems in the Milky Way Galaxy.

In Sect. 2 we describe the *Chandra* data and analysis, followed by a description of our findings in Sect. 3. We discuss our results in Sect. 4.

2. Observations and data analysis

The 30 Doradus region was observed with *Chandra* for 21 ksec on 2000 Sep 13 with the Advanced CCD Imaging Spectrometer-Imager (ACIS-I), a $16'9 \times 16'9$ array of four front-side illuminated CCDs (Garmire, Nousek, & Bautz in preparation). The R 136 star cluster was at the telescope's aim point. The data were taken in timed-exposure (TE) mode using the standard integration time of 3.2 sec per frame and telemetered to the ground in very faint (VF) mode. See the *Chandra* Proposers' Observatory Guide for details (*Chandra* website <http://asc.harvard.edu/>).

We followed the data preparation threads provided by the *Chandra* team and given on their website. We used the *Chandra* Interactive Analysis of Observations (CIAO) software package to perform the reductions, with the most up-to-date (as of June 2001) calibration files (gain maps, quantum efficiency, quantum efficiency uniformity, effective area) available for this observation. Bad pixels were excluded. Intervals of bad aspect and intervals of background flaring¹ were searched for, but none were found.

To detect sources, we first filtered the unprocessed data to exclude software-flagged cosmic ray events and then processed the data without including the pixel randomization that is added during standard processing. This custom processing slightly improves the point spread function (PSF). We then used the CIAO tool *wavdetect*, a wavelet based source detection program. We found 30 point sources and two extended sources (SNR 0538-69.1 and an unidentified one) in the entire ACIS-I field. Fig. 1 shows a $11' \times 11'$ image (left) and a blow up of the central $7''$ square (right) *Chandra* image with the source names identified. The names of the sources correspond to the 20 sources listed in Tab. 1.

¹See http://asc.harvard.edu/cal/Links/Acis/acis/Cal_prods/bkgrnd/current for a discussion of background flares.

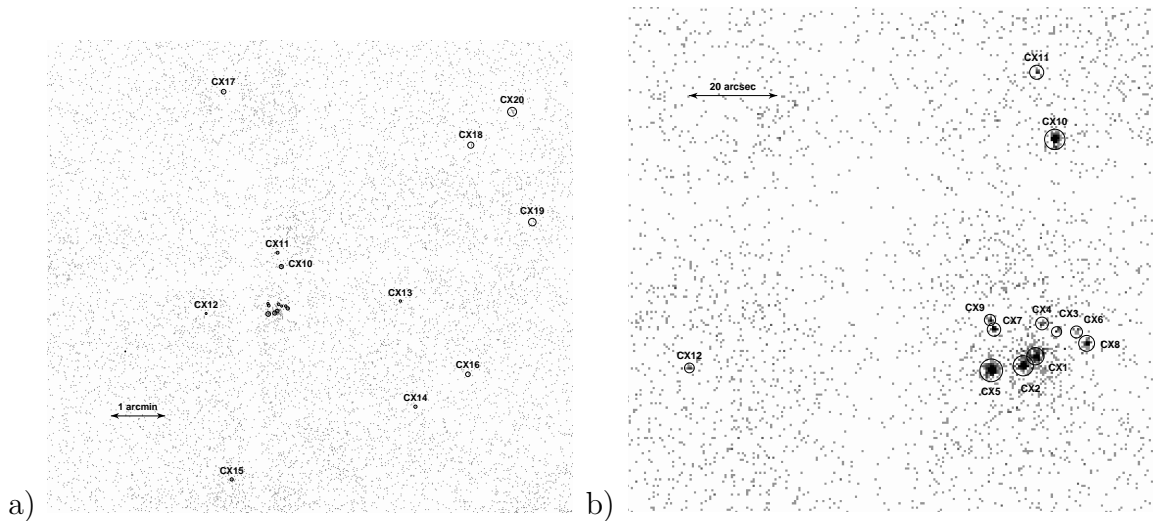


Fig. 1.— X-ray image of the star cluster R 136 in the 30 Doradus region. a) $11' \times 11'$ view, b) close up of the cluster. The sources are identified in Tab 1.

Radial surface brightness profiles were constructed for the four brightest sources and compared to expected PSF profiles for those chip locations. Only CX10 (near the star cluster R 140) was inconsistent with a point source (3.4σ).

The positions listed in Tab. 1 are the *wavdetect* centroid positions based on the *Chandra* astrometric solution. The uncertainties range from $\sim 0''.1$ for the brighter sources to $\sim 1''$ for the dimmer sources. To perform source identifications, we used Parker’s catalog of bright stars in the 30 Doradus region (Parker 1993). These positions are accurate within $0''.4$. Registration of the *Chandra* frame of reference with the Parker frame was accomplished via a uniform shift calculated from a least-squares best fit to the offsets from nearby optical sources of eight X-ray sources (CX2, CX4, CX5, CX6, CX7, CX8, CX12 and CX19), six in the central region and two outside the central region. In a similar manner, the Parker frame was registered with the *Hubble* frame by a uniform shift based on five stars (names from Parker 1993: 1120, 1134, 922, 786, 767) in the central region. The Parker-to-*Hubble* shift was $0''.07$ in RA (true arcsec) and $-1''.32$ in Dec. The total *Chandra*-to-*Hubble* shift was $1''.35$ in RA (true arcsec) and $0''.66$ in Dec. Fig. 2 shows the *Chandra* sources (ellipses) and Parker stars (boxes) overlaid on a *Hubble* image of the central region. The sizes of the ellipses and boxes indicate the 1σ position errors.

X-ray spectra of the 5 brightest *Chandra* sources were extracted with the CIAO tool *dmextract*. Spectral fitting (using χ^2 statistics) was done in XSPEC with the data grouped to ≥ 10 counts per bin for CX1 and CX8, ≥ 20 counts per bin for CX2 and CX10, and ≥ 30 counts per bin for CX5. Because of the association of nearly all the X-ray sources with

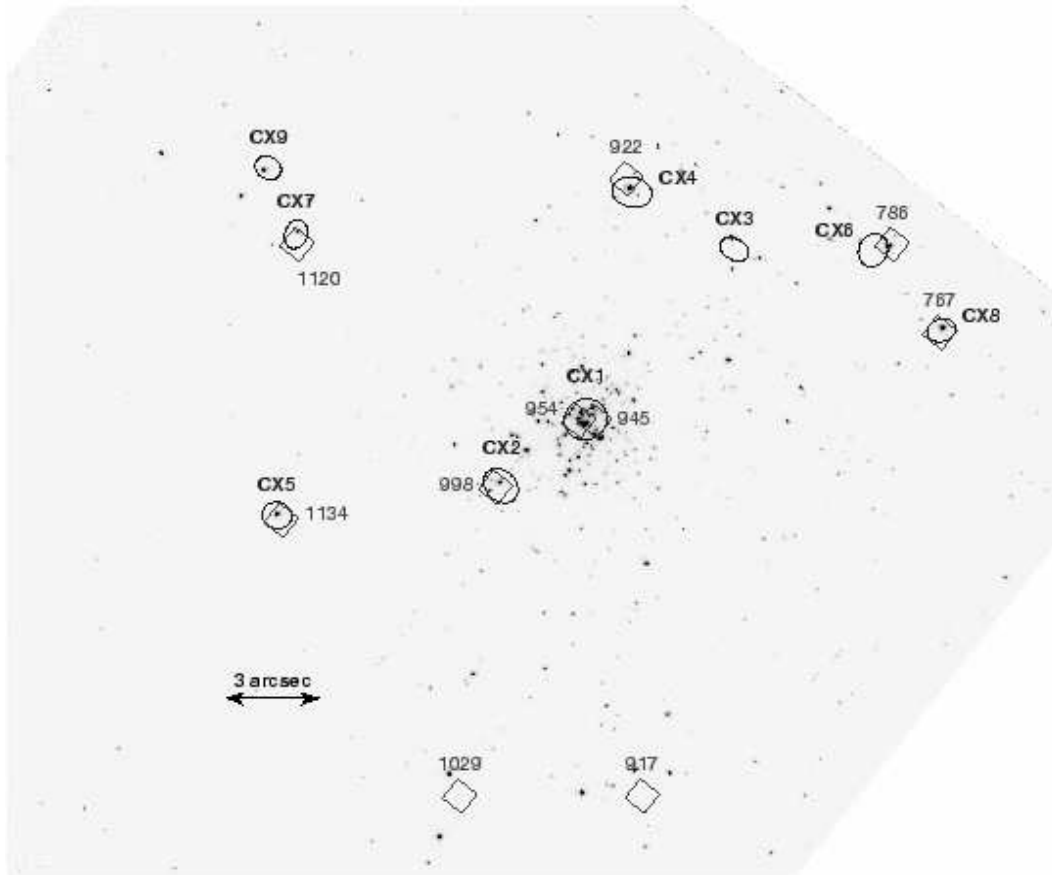


Fig. 2.— Hubble Space Telescope image of R 136, the central portion of the 30 Doradus region (Massey & Hunter 1998). The exposure time was 26 seconds with filter F336W (centered on 3344 \AA , and with a 381 \AA bandpass) using WFPC2. The Wolf-Rayet stars identified by Parker (1993) are indicated by squares and the ellipses give the locations of the Chandra X-ray sources (see Tab.1 and 2). The sizes of the ellipses give the 1σ positional accuracy for the *Chandra* sources.

Table 1: *Chandra* detections of X-ray point sources near the star cluster R136. RA: $5^h38^m43^s.2$, Dec: $69^\circ6'0''$ in the year 2000AD. Columns give the name of the source, its position in RA and Dec, the distance to the star R136a (CX1), number of counts in 0.3–8.0 keV, the fit parameters kT_{mekal} and n_H , the Chi-squared χ^2 statistic and degrees of freedom (dof), and the unabsorbed luminosity in the 0.2 to 3.5 keV *Einstein* band. For sources with $\lesssim 90$ counts (including CX20 because of the lack of an optical counterpart) we estimate the luminosities based on a best-fit linear relation between counts and luminosities for four of the five brightest sources (we excluded CX10, see sect. 2).

Source	RA	Dec	r [$''$]	Counts	kT_{mekal} [keV]	n_H [10^{21} cm^{-2}]	χ^2/dof	$\log L_{0.2-3.5\text{keV}}$ [erg s^{-1}]
CX1	05:38:42.210	-69:06:03.85	0	146	1.7	2.8	14.6/13	34.34
CX2	05:38:42.722	-69:06:06.02	3.5	390	2.1	6.3	19.7/18	34.93
CX3	05:38:41.311	-69:05:58.30	7.3	13				33.17
CX4	05:38:41.930	-69:05:56.43	7.6	16				33.31
CX5	05:38:44.077	-69:06:07.05	10.5	997	3.3	4.8	33.0/32	35.26
CX6	05:38:40.470	-69:05:58.34	10.8	9				32.86
CX7	05:38:43.962	-69:05:57.81	11.2	51				33.93
CX8	05:38:40.042	-69:06:00.94	12.0	91	2.1	1.6	8.0/6	34.00
CX9	05:38:44.130	-69:05:55.64	13.2	20				33.44
CX10	05:38:41.391	-69:05:14.67	49.4	374	1.1	7.9	11.4/17	35.22
CX11	05:38:42.156	-69:04:59.46	64.4	17				33.35
CX12	05:38:56.852	-69:06:06.48	78.4	11				33.04
CX13	05:38:16.909	-69:05:52.57	136	6				32.23
CX14	05:38:13.755	-69:07:49.13	185	7				32.55
CX15	05:38:51.602	-69:09:09.59	192	15				33.27
CX16	05:38:02.963	-69:07:13.28	221	8				32.73
CX17	05:38:53.226	-69:02:01.82	249	13				33.17
CX18	05:38:02.508	-69:03:00.44	281	22				33.50
CX19	05:37:49.811	-69:04:25.14	297	17				33.35
CX20	05:37:54.057	-69:02:23.54	339	94				34.22

Wolf-Rayet stars, we chose the *mekal* model (Mewe et al. 1985) with absorption, which fits better than thermal bremsstrahlung models. A summary of the results is given in Tab.1. The spectra of the brightest two sources (CX2 and CX5), which are quite representative, are shown in Fig. 3. For a better comparison with previous observations, which were mostly done with the *Einstein* observatory, we calculate the luminosities over the same band. Though a source can be detected with only a few counts, $\gtrsim 100$ counts are required to fit a spectrum with any confidence. To estimate the luminosity of the dimmer sources, we use a best-fit linear relationship between observed counts and unabsorbed luminosities for four of the brightest five sources. Because the source CX10 is bright for its count rate and extended, we excluded it when deriving this relation.

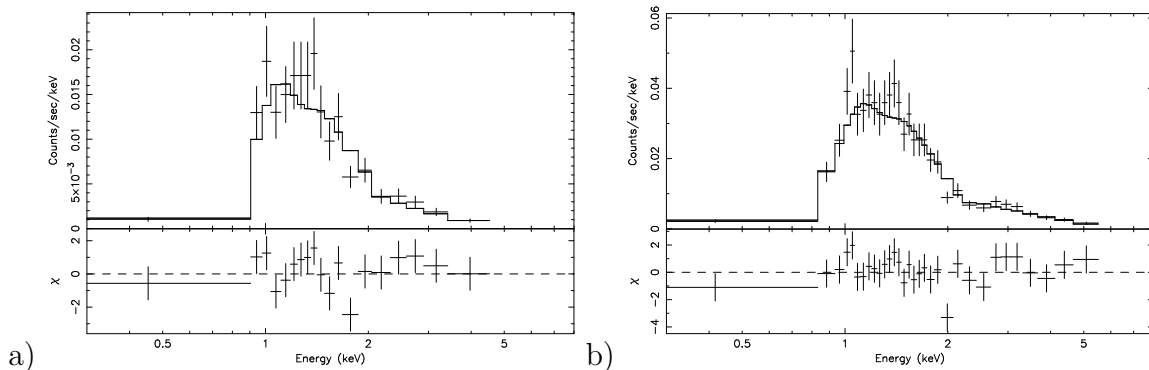


Fig. 3.— X-ray spectra of the two brightest sources CX2 (a) and CX5 (b). The data (crosses) and best-fit *mekal* model (solid line) are shown in both panels. The lower panels give the contribution to the χ^2 statistics for each bin.

We identify source CX10 with W5 and CX5 with W7 from Wang (1995). The luminosities for these two sources calculated from our best fit models are lower than those of Wang by a factor of ~ 10 , but this is somewhat deceptive. Wang used multicolor blackbody disk models (MBD) with absorption and could only fit over the 0.5–2 keV *ROSAT* band. Such models do not fit our broader band (0.3–8 keV) data well. If we restrict our data to the *ROSAT* band, we find that MBD models fit the data, but the column densities required for good fits with these models are much higher than those required for fits with the *mekal* model. When we calculate *intrinsic* source luminosities based on MBD fits to the 0.5–2 keV *Chandra* data, our results are consistent with those of Wang. There is no evidence for variability on the time scale between the two observations 9 years apart. Also, none of our sources show statistically significant variability during the *Chandra* observation.

3. Results and interpretation

3.1. Optical counterparts

We concentrate on the 11 X-ray sources (CX1–CX11) which are located within $100''$ (~ 25 pc in projection at a distance of 51 kpc) from the central star R 136a1 of the star cluster R 136. For the other eight sources we have insufficient information to include them in our study. Two of these remaining sources (CX12 and CX17) have a WN type Wolf-Rayet star as optical counterparts (see Tab. 2), CX14 is an IRAS source and CX19 has the foreground star MH 2 as counter part (Fehrenback and Duflot, 1970), which is observed in infrared (McGregor & Hyland, 1981) and classified as a spectral type M star (Hyland, Thomas & Robinson 1978). The remaining five sources (CX13, CX15, CX16, CX18 and CX20) are not identified.

All 11 sources (CX1 to CX11) have a bright optical star within the 1σ error ellipse of the corrected *Chandra* position. Fig. 2 gives a *Hubble Space Telescope* image of R 136 (Massey & Hunter 1998). The ellipses indicate the 1σ error at the location of our 11 *Chandra* point sources near R 136. Details about these sources are given in Tab. 1.

Parker (1993) identifies 12 WN type Wolf-Rayet stars (see Tab. 2) near the star cluster R 136. These are identified in Fig. 2 by squares. Five of these (R 136a1, a2, a3, a5 and R 136b) are embedded deep in the core of the cluster. The source CX10 has the small cluster R 140 as counterpart, which is at about 11.5 pc in projection to the north of R 136a. This cluster contains at least two WN stars and one WC star (Moffat 1987). We found CX10 to be extended and it may well be a blend of several colliding wind binaries.

Seven of nine of the remaining sources have WN stars as counterparts, and the other two coincide with spectral type O3f* stars (Crowther & Dessart, 1998). Melnick (1978 see also Melnick 1985 and Bosch et al. 1999) lists most of the Wolf-Rayet stars (and one of the O3f* stars which are associated with our X-ray sources) as binaries with a spectral type O or B companion. The four exceptions P860, Mk39, R134 and R139 are not known to be binaries. The star Mk33Na is listed as a binary by Crowther & Dessart (1998) but not by Melnick (1978; 1985). The two stars R 144 and R 145, which are associated with CX17 and CX12, respectively, are little discussed in the literature, both are WN6h stars (Crowther & Smith 1997).

Tab. 2 lists the X-ray sources and their counterparts.

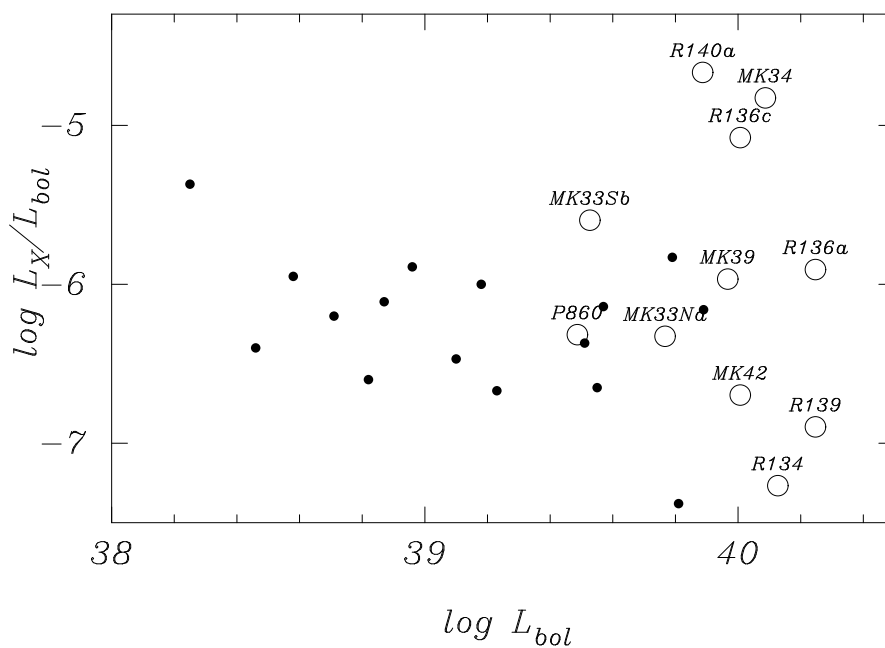


Fig. 4.— Ratio of the X-ray luminosity (0.2 – 3.5 keV) to the Bolometric luminosity (L_X/L_{bol} for the X-ray sources from Tab. 2 and Tab. 3 as a function of the Bolometric luminosity (in ergs^{-1}). The known Galactic colliding wind binaries from Tab. 3 are indicated with bullets (see Fig. 5 for the error bars). The sources from Tab. 2 are indicated by circles and identified by the names of their optical counterparts. Note that the two types of sources (Galactic versus those near NGC 2070) are selected on different criteria and a direct comparison has to be carried out with care.

3.2. The nature of the X-ray sources

We now study the possibility that the X-rays are produced in the stellar winds in the optical counterparts. Wolf-Rayet stars are known to be bright X-ray sources (Pallavicini et al. 1981), which follow the empirical relation between X-ray and Bolometric luminosity of $L_X/L_{\text{bol}} \simeq 10^{-7 \pm 1}$. This relation holds for a wide range of stellar spectral types down to late B. White & Long (1986) confirm the existence of this relation for WN and WC type Wolf-Rayet stars. An extensive study by Pollock (1987) using the *Einstein* observatory confirms this relation for binaries with a WN or WC Wolf-Rayet star as primary.

The sample of Chlebowski & Garmany (1991) contains early type O stars, which may follow a different relation between L_X and L_{bol} than Wolf-Rayet stars. However, the Wolf-Rayet stars listed by White & Long (1986, 2 WN and 4 WC stars) and by Pollock (1987, 7 WN and 4 WC stars) follow the same relation as the early type O stars of Chlebowski & Garmany (1991). (To minimize confusion we decided to show only the stars listed by Chlebowski & Garmany in Fig. 4.)

In Fig. 4 we compare the relation between Bolometric luminosity L_{bol} and L_X/L_{bol} of 11 of our observed X-ray sources with that of the 16 X-ray bright stars in the sample discussed by Chlebowski & Garmany (1991). To make the comparison, we calculate the 0.5–3.5 keV luminosity from our best-fit models (which were fit over the entire 0.3–8.0 keV *Chandra* band) since this was the band used by Chlebowski & Garmany (1991), who observed with the *Einstein* observatory (see Tab. 1). Between the stars in NGC 2070 and the sample of Chlebowski & Garmany (1991), three stars (R140a, Mk34 and R136c) are considerably brighter than expected from the empirical relation, and the scatter among the stars in NGC 2070 is larger than for the sample of Galactic sources. The unusual brightness of CX10 may be explained as a blend of several objects in the sub cluster R140.

We have no ready explanation for the extreme brightness of the other two stars, but bear in mind that the stars associated with our X-ray sources are unusually bright and massive, ranging from $50 M_{\odot}$ to $150 M_{\odot}$ (see Tab. 2), unlike any stars in the Milky Way Galaxy. It is therefore possible that they do not follow the same relation as the rather “low” mass ($15 M_{\odot}$ to $30 M_{\odot}$) stars in the Milky Way Galaxy. Note also that a direct comparison between the Galactic X-ray sources and those near NGC 2070 has to be carried out with care as both have been selected on different grounds.

3.3. X-rays from colliding stellar winds

The typical mass loss rate for a WN Wolf-Rayet star is between 10^{-5} and 10^{-4} $M_{\odot} \text{ yr}^{-1}$ and somewhat smaller for an Of* star (see Tab. 2). When the fast mass outflow of one of these stars collides with the mass outflow of a companion star, strong shocks form. For a single star, the shocks will be much weaker because the relative velocity of the shocked material is much smaller for a single star than one in a binary. The temperature in the shocks can be very high, at which point X-rays are produced (Prilutskii & Usov 1976; Cherepashchuk 1976; Cooke, Fabian & Pringle 1978). The X-ray emission observed from such systems is generally rather soft ($kT \sim 1 \text{ keV}$), originating from the outer parts of the wind (Pollock 1987).

We estimate the total X-ray luminosity in the colliding wind in the limit of completely isothermal radiative shocks and assuming that the flow is adiabatic². The total X-ray luminosity is given by the product of the emissivity per unit volume, $n^2\Lambda$, with the volume of the shock-heated wind. Here $\Lambda \propto T^{-0.6}$ is the emission rate at which the gas cools (see Stevens, Blondin & Pollock 1992). In the adiabatic limit for a binary star with orbital separation $a \gg r$ the volume of the shock heated gas scales as a^3 . Here r is the stellar radius. The density $n \propto \dot{m}_{\text{wind}}/(a^2 v_{\text{wind}})$. The total luminosity due to the shock is then $L \propto \dot{m}_{\text{wind}}^2/(v_{\text{wind}}^2 a)$. We assume that the post shock temperature equals the temperature on the line connecting the two stars and using $T \propto v_{\text{wind}}^2$, and define (in cgs units):

$$S_X = \frac{\dot{m}_{\text{wind}}^2}{v_{\text{wind}}^{3.2} a}. \quad (1)$$

Here we assume momentum balance of the two winds on the connecting lines between the two stars, i.e., the two stars are equally windy (equipetomaniac). This relation has been tested with detailed calculations by Luo, McCray & Mac Low (1990) and Stevens, Blondin & Pollock (1992).

We will now calculate the terminal velocity of the stellar wind of early type O stars and Wolf-Rayet stars. The luminosity L of massive main-sequence stars $L \propto m^3$ and the radius $r \propto m$. With $L \propto r^2 T_{\text{eff}}^4$ and the escape velocity from the stellar surface $v_{\text{esc}}^2 \propto m/r$ we can write $v_{\text{esc}} \propto T_{\text{eff}}/m^{1/4}$, i.e., the escape velocity of a massive star is proportional to its effective temperature. The terminal velocity in the stellar wind $v_{\infty} \propto v_{\text{esc}}$. However, the velocity of the stellar wind at the moment it collides may be smaller than the escape velocity from the stellar surface, but larger than the terminal velocity. We write the velocity

²We refer to the total X-ray luminosity as our model is too simple to identify any energy dependency.

at the moment the winds collide as

$$v_{\text{wind}} = v_{\infty} \left(1 - \frac{r}{a}\right) \quad (2)$$

For simplicity we assume that the winds collide at distance a from the primary star with radius r , which we calculate from the effective temperature and the luminosity.

We calibrate the relation between the terminal velocity and the stellar temperature with the list of O and B stars in Tab. 3, which results in

$$v_{\infty} \simeq 130 \frac{T_{\text{eff}}}{[1000K]} - 2800 [\text{km s}^{-1}], \quad (3)$$

For the O stars in our sample we can apply the same relation between the wind velocity and the effective temperature of the star. For Wolf-Rayet stars, however, this relation breaks down³.

Crowther & Dessart (1998) list mass loss rates, \dot{m}_{wind} and Bolometric luminosities L_{bol} for most of the optical counterparts to our X-ray sources but not their terminal velocities. We derive the escape velocity v_{ce} from the core of a Wolf-Rayet star using its luminosity. The terminal velocity then follows from the empirical relation of Nugis & Lamers (2000). The wind velocity is then calculated using Eq. 2.

The terminal velocity v_{∞} is given by (Nugis & Lamers 2000)

$$\log v_{\infty}/v_{\text{ce}} \simeq 0.61 - 0.13 \log \mathcal{L} + 0.3 \log Y. \quad (4)$$

We define the luminosity $\mathcal{L} \equiv L/L_{\odot}$, mass $\mathcal{M} \equiv m/M_{\odot}$ and radius $\mathcal{R} \equiv r/R_{\odot}$ of the core of the Wolf-Rayet star in solar units. Y is the Helium mass fraction of the star.

The effective escape velocity from the stellar core is

$$v_{\text{ce}} \simeq 438 \sqrt{\frac{\mathcal{M}(1 - \Gamma_e)}{\mathcal{R}}} \quad [\text{km s}^{-1}] \quad (5)$$

Here $\Gamma_e \simeq 7.66 \times 10^{-5} \sigma_e \mathcal{L} / \mathcal{M}$, corrects the gravity for electron scattering, and the electron scattering coefficient is $\sigma_e \simeq 0.4(X + \frac{1}{2}Y + \frac{1}{4}Z) \text{ cm}^2$ (see Nugis & Lamers, 2000).

The core radius is given by

$$\log \mathcal{R} \simeq -1.845 + 0.338 \log \mathcal{L}. \quad (6)$$

³The radius of a Wolf-Rayet star is ill defined because the wind is optically thick due to the large mass loss rate; the stellar radius depends on the wavelength. The effective temperature of a Wolf-Rayet star is therefore ill defined.

The mass is obtained by iterating the mass-luminosity relation for massive Wolf-Rayet stars (Schaerer & Maeder 1992)

$$\log \mathcal{L} \simeq 2.782 + 2.695 \log \mathcal{M} - 0.461 (\log \mathcal{M})^2. \quad (7)$$

The $L - v_{ce}$ relation derived with this model fits well with WN4 to WN6 stars of Hamann & Koesterke (2000), the cores of planetary nebulae of Kudritzki & Puls (2000) and with the sample of 24 Galactic and 14 Magellanic Cloud O stars of Puls et al. (1996).

Fig. 5 shows the results of Eq. 1 with S_X along the horizontal axis and the observed X-ray luminosity in the Einstein band along the vertical axis. The bullets indicate the locations of the 16 colliding wind Wolf-Rayet binaries from Chlebowski & Garmany (1991). The orbital separation for these binaries is calculated using Keplers' third law with the mass and orbital period given by Chlebowski & Garmany (1991). When no mass estimate is provided we assume a total binary mass of $30 \pm 15 M_\odot$. A fit to this data is presented as the solid line in Fig. 5, which represents

$$L_X = 10^{33.0 \pm 0.2} S_X^{0.2 \pm 0.1}, \quad (8)$$

where the dotted lines gives the uncertainty interval.

The names of the optical counterparts of the X-ray sources from Tab. 2 are plotted in Fig. 5. The value of S_X for these stars is calculated with Eq. 1 assuming that they are binaries with an orbital separation of $100 R_\odot$. For the wind velocity in Eq. 1, we adopt both extremes, the terminal velocity and the escape velocity from the Wolf-Rayet star. The uncertainty thus obtained is proportional to the size of the name tags in Fig. 5. Only the orbital period of R 140a is known (2.76 days; Moffat et al. 1987). With a total binary mass of about $100 M_\odot$, this period corresponds to an orbital separation of about $40 R_\odot$. The accurate orbital separation is not crucial for our crude model as it enters only linearly in Eq. 1. However, when the orbital separation becomes comparable to the size of the primary (windy) star, the wind velocity v_{wind} may strongly deviate from the terminal wind velocity (via Eq. 2). (Our assumption that binary members are equipotential and equally massive, has obviously limited validity.)

4. Discussion

We have analyzed archival *Chandra* data of the central portion of the 30 Doradus region including the star clusters R 136 and R 140.

We confirm the detection of two bright X-ray sources with the stars Mk34 and R 140a as optical counterparts (see Wang & Helfand 1991). The X-ray luminosities of these two

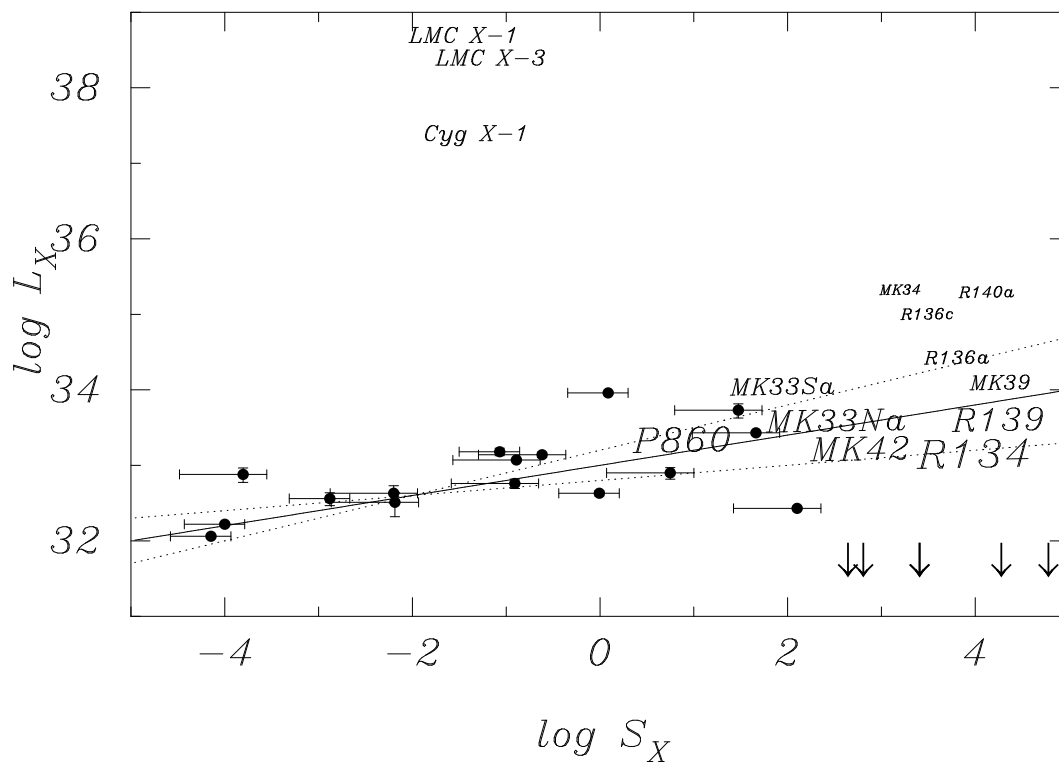


Fig. 5.— X-ray luminosity as a function of S_X (Eq. 1). The bullets give the location of the binaries listed by Chlebowski & Garmany (1991). The *Chandra* X-ray sources from Tab. 2 are identified by their optical counterpart; the size of their names are proportional to the 1σ errors. The solid line gives a least squares fit to the bullets, which represent the sources of Tab. 3. The dotted lines represent the uncertainty interval of the fit. For comparison we plot the location of three known high-mass X-ray binaries with a black hole (see discussion). The value of S_X (Eq. 1) for the five down pointed arrows represent the stars (from left to right) R136b, Mk37Wb, Mk35, Mk30 and Mk49, which we did not detect in X-rays.

Table 3: Parameters for known black hole X-ray binaries and X-ray sources with early type stars as optical counterparts. The first three entries are the black hole X-ray binaries (Gies & Bolton (1982), and Lui et al. 2000). The following 16 sources are X-ray luminous O and B stars observed with *Einstein*. The X-ray data is taken from Chlebowski, Harnden & Sciortino (1989). Temperature, luminosity, mass loss rate, and wind velocities are from Chlebowski & Garmany (1991).

name	Spectral type	P_{orb} [days]	T_{eff} [1000K]	$\log L_{\text{bol}}$ [erg s^{-1}]	$\log L_X$	N_{counts}	$\log \dot{m}_{\text{wind}}$ [$M_{\odot} \text{ yr}^{-1}$]	v_{∞} [km/s]
Cyg X-1	O9.7ab	5.6			37.3	var.	-7.0	1800
LMC X-1	O7–9II	4.2			38.6	var.	-7.0	2100
LMC X-3	B3V	2.3			38.6	var.	-8.0	490
HD 1337	O9III	3.52	34.0	39.55	32.90	32.8	-6.17	2200
HD 12323	ON9	3.07	35.9	38.25	32.88	21.1	-8.37	1300
HD 37041	O9V	20.79	35.9	38.46	32.06	305	-8.24	1700
HD 37468	O8.5III	30	35.0	38.82	32.22	681	-8.14	1300
HD 57060	O7Ia	4.39	36.1	39.81	32.43	534	-5.35	1800
HD 75759	O9Vn	33.31	35.9	39.23	32.56	26.8	-7.49	1600
HD 93206	O9.7Ib	6	30.6	39.57	33.43	327	-5.85	2500
HD 93205	O3V	6.08	48.5	39.51	33.14	144	-6.23	3600
HD 93403	O5III	15.09	42.3	39.79	33.96	667	-5.82	3000
HD 100213	O8.5	1.39	37.0	38.58	32.63	15.1	-7.65	1800
HD 152218	O9.5IV	5.40	34.0	38.87	32.76	48.9	-6.93	3000
HD 152590	O7.5V	4.49	39.1	38.71	32.51	7.95	-7.36	2300
HD 159176	O7V	3.37	40.1	38.96	33.07	859	-6.72	2600
HD 165052	O6.5V	6.14	41.2	39.18	33.18	77.5	-6.62	2700
HD 206267	O6.5V	3.71	41.2	39.10	32.63	120	-6.16	3100
HD 215835	O6V	2.11	42.2	39.89	33.73	22.1	-5.54	3350

sources have not noticeably changed in the 9 years between observations. The difference in X-ray luminosity between the earlier observation and ours can be attributed to the different spectral fitting.

We identified 20 point sources with an X-ray luminosity ranging from 5×10^{32} to $2 \times 10^{35} \text{ erg s}^{-1}$. Nine point sources are located within $14''$ (3.4 pc) of the center of the star cluster R 136, one possibly extended source is associated with the cluster of WN stars R 140. Four others have WN stars as counterparts which do not seem to be associated with either of the two clusters.

Wang (1995) analyzed ROSAT spectra of our sources CX5 (his source number 7) and CX10 (his number 5). He concluded that they are probably high-mass X-ray binaries with a black hole as accreting star. His arguments are based on the spectral temperature (0.1–0.2 keV for his source number 5 and 0.2–0.4 keV for number 7) and the high luminosity ($\sim 10^{36} \text{ erg s}^{-1}$). In addition he uses the measured orbital period of 2.76 days and mass function of $0.12 M_{\odot}$ of the star R 140a2 (see Moffat et al. 1987) as an argument for the presence of a dark object.

For comparison we calculate the value of S_X (Eq. 1) for the three known black hole X-ray binaries (see Tab. 3) and plot these in Fig. 5. Their positions in Fig. 5 are completely different from the X-ray sources in NGC 2070. Of course, there is an interpretational difficulty here about which state of the black hole binary (see Tanaka & Lewin 1995) should be used for a comparison. In any case, the age of the cluster would make it remarkable if any of the X-ray sources were associated with a black hole or a neutron star. On these grounds we conclude that none of the X-ray sources in NGC 2070 are associated with compact objects.

We conclude that all sources are consistent with colliding wind systems. X-rays are produced in the collisions between the winds in close binaries in which these stars reside. We derive an empirical relation for the X-ray luminosity for a colliding wind binary by substitution of Eq. 1 in Eq. 8:

$$L_x = 1.3 \times 10^{34} \left(\frac{\dot{m}_{\text{wind}}}{10^{-5} M_{\odot} \text{yr}^{-1}} \right)^{0.4} \left(\frac{1000 \text{ km s}^{-1}}{v_{\text{wind}}} \right)^{0.65} \left(\frac{R_{\odot}}{a} \right)^{0.20} \text{ [erg s}^{-1}] \quad (9)$$

This relation has a weaker dependence on the velocity and orbital separation compared to Usov’s (1992) theoretical expression (his Eq. 89).

About 70 % (13/18) of the Wolf-Rayet stars in NGC 2070 are bright in X-rays. The star cluster also contains 5 spectral type O3f* and WN stars (R 136b, Mk37Wb, Mk35, Mk30 and Mk49) which do not show up in our X-ray image. Using Eq. 9 one would expect X-ray fluxes at least an order of magnitude above our detection threshold of $5 \times 10^{32} \text{ erg s}^{-1}$

(see down pointed arrows in Fig. 5). The absence of X-rays for these stars can be explained by the companion mass being much smaller than that of the WN star or by the orbital separation being much larger than the adopted $100 R_{\odot}$. Alternatively, these stars are single, in which case they may be much dimmer in X-rays.

The star cluster NGC 3603 has characteristics similar to R 136, and therefore may also host a wealth of X-ray sources. As suggested by the referee, we examined the public 50 ks *Chandra* data centered on NGC 3603, but it goes beyond the scope of this paper to fully reduce and analyze these data. The cluster shows a wealth of interesting features including diffuse X-ray emission, exceptionally bright point sources and a large number of much dimmer point sources (Moffat, Corcoran, Stevens, Skalkowski, Marchenko, Müke, Ptak, Koribalski, Mushotzky, Pittard, Pollock and Brandner, 2002 in preparation and Stevens, private communication). The sources in the cluster center are heavily blend and it will be a very time-consuming task to find optical counterparts.

Other clusters with similar characteristics as R 136 are the Arches, the Quintuplet cluster and Westerlund 1. These clusters also contain a wealth of bright and young early spectral types star which, when in binaries, may be bright X-ray point sources with characteristics similar to those discussed in relation to R 136.

5. Conclusions

We analyzed a 21 ksec archival *Chandra* X-ray observation pointed at the central portion of the 30 Doradus region in the Large Magellanic Cloud. The image contains 18 new X-ray sources and we confirm the existence of two sources earlier discovered by Wang & Helfand (1991). Nine sources are within ~ 3.4 pc of the center of the young star cluster R 136. The X-ray luminosity (0.2 – 3.5 keV) of these sources ranges from 5×10^{32} (our detection threshold) to 2×10^{35} erg s $^{-1}$. The two known sources have not changed noticeably in X-ray luminosity over the 9 years between the *Einstein* and our *Chandra* observations.

We conclude that all observed sources, except for 5 unidentified sources, the IRAS source IRS 2, and the foreground infrared source MH 2, have stars as counterparts (10 WN Wolf-Rayet, two Of* and one O3V star). We argue that the X-rays in these stars are produced by colliding winds.

We do not agree with Wang (1995) that the two earlier discovered sources (CX5 and CX10) host black holes because 1) the stellar environment is too young to produce black holes, 2) the spectra and X-ray luminosities of the sources do not at all agree with other known black hole candidates, and 3) the sources fit well with our simple semi-analytic

colliding wind model.

The X-ray luminosities of the other observed sources agree well with our simple colliding wind model. The model gives the X-ray luminosity as a function of the stellar wind mass loss, its terminal velocity and the binary separation. The empirical fit, calibrated to 16 known colliding wind binaries, culminates in Eq. 9.

This empirical relation can be used to reduce the noise in the relation between the 0.2 to 3.5 keV X-ray luminosity and the Bolometric luminosity of early type stars. The luminosity calculated with Eq. 9 provides a powerful diagnostic for studying colliding wind X-ray binaries.

If the X-rays are indeed the result of colliding winds in close binaries, possibly all 13 identified sources detected with *Chandra* could be close binaries. In that case we conclude that the binary fraction among early type stars in the 30 Doradus region is unusually high; possibly all early type stars are binaries.

Other star clusters, with age, mass and concentration similar to R 136 are likely to contain a similar wealth in bright X-ray sources. In these cases, the emission may also be produced by colliding stellar winds. We then conclude that the star cluster NGC 3603 may contain more than 20 X-ray sources brighter than 10^{33} ergs $^{-1}$ but the majority may be blended in the cluster center. (Preliminary results of an X-ray study with *Chandra* were reported at the AAS December meeting by Corcoran et al., 2000, Moffat et al. 2002 in preparation)

We are grateful to Ron Remillard and Ian Stevens for discussions. This work was supported by NASA through Hubble Fellowship grant HF-01112.01-98A awarded (to SPZ) by the Space Telescope Science Institute and by the Royal Dutch Academy of Sciences (KNAW). DP acknowledges that this material is based upon work partially supported under a National Science Foundation Graduate Fellowship.

REFERENCES

- Bosch, G., Terlevich, R., Melnick, J., Selman, F. 1999, A&AS, 137, 21
- Brandl, B., Brandner, W., Eisenhauer, F., Moffat, A. F. J., Palla, F., Zinnecker, H. 1999, A&A, 352, L69
- Brandl, B., Sams, B. J., Bertoldi, F., Eckart, A., Genzel, R., Drapatz, S., Hofmann, R., Loewe, M., Quirrenbach, A. 1996, ApJ, 466, 254

- Campbell, B., Hunter, D. A., Holtzman, J. A., Lauer, T. R., Shayer, E. J., Code, A., Faber, S. M., Groth, E. J., Light, R. M., Lynds, R., O’Neil, E. J., J., Westphal, J. A. 1992, AJ, 104, 1721
- Cassinelli, J. P., Mathis, J. S., Savage, B. D. 1981, Science, 212, 1497
- Cherepashchuk, A.M., 1976, Sov. Astr. 2, L138
- Chlebowski, T., Harnden, F. R., Sciortino, S. 1989, ApJ, 341, 427
- Corcoran, M. F., Moffat, A., Mushotzky, R., Stevens, I. R., Muecke, A., Skalkowski, G., Brandner, W., Koribalski, B., Marchenko, S., Ptak, A., Pollock, A. M. T., Koenigsberger, G., 2000, AAS Meeting 197, #38.15
- Cooke, B. A., Fabian, A. C., Pringle, J. E. 1978, Nature, 273, 645
- Crowther, P. A., Dessart, L. 1998, MNRAS, 296, 622
- Crowther, P. A., Smith, L. J. 1997, A&A, 320, 500
- de Koter, A., Heap, S. R., Hubeny, I. 1997, ApJ, 477, 792
- Dennerl, K., Haberl, F., Aschenbach, B., Briel, U. G., Balasini, M., Bräuninger, H., Burkert, W., Hartmann, R., Hartner, G., Hasinger, G., Kemmer, J., Kendziorra, E., Kirsch, M., Krause, N., Kuster, M., Lumb, D., Massa, P., Meidinger, N., Pfeffermann, E., Pietsch, W., Reppin, C., Soltau, H., Staubert, R., Strüder, L., Trümper, J., Turner, M., Villa, G., Zavlin, V. E., 2001, A&A 365, L202
- Fehrenback, C., & Duflot, M., 1970, AASS, Ser. 1, 1
- Feigelson, E. D., 2000, To appear in *X-ray Astronomy 2000* (eds. R. Giacconi, L. Stella & S. Serio) (astro-ph/0012486)
- Gies, D. R., Bolton, C. T. 1982, ApJ, 260, 240
- Hamann, W. ., Koesterke, L. 2000, A&A, 360, 647
- Hyland, H. R., Thomas, J. A. & Robinson, G., 1978, AJ, 80, 20
- King, I. R., 1966, AJ, 71, 64
- Kudritzki, R., Puls, J. 2000, ARA&A, 38, 613
- Liu, Q. Z., van Paradijs, J., van den Heuvel, E. P. J. 2000, A&AS, 147, 25

- Luo, D., McCray, R., Mac Low, M., 1990, ApJ 362, 267
- Massey, P., Hunter, D. A. 1998, ApJ, 493, 180
- McGregor, P. J., & Hyland, A. R., 1981, ApJ, 250, 116
- Melnick, J. 1978, A&AS, 34, 383
- Melnick, J. 1985, A&A, 153, 235
- Mewe, R., Gronenschild, E.H.B.M., and van den Oord, G.H.J. 1985, A&AS, 62, 197
- Meynet, G., Maeder, A., Schaller, G., Schaerer, D., Charbonnel, C. 1994, A&AS, 103, 97
- Moffat, A. F. J., Niemela, V. S., Phillips, M. M., Chu, Y., & Seggewiss, W., 1987, ApJ, 312, 612
- Moffat, A. F. J., Drissen, L., Shara, M. M. 1994, ApJ, 436, 183
- Nagata, T., Woodward, C. E., Shure, M., Kobayashi, N. 1995, AJ, 109, 1676
- Nagata, T., Woodward, C. E., Shure, M., Pipher, J. L., Okuda, H. 1990, ApJ, 351, 83
- Nugis, T. & Lamers, H. J. G. L. M., 2000, *a*, 360, 227,
- Okuda, H., Shibai, H., Nakagawa, T., Matsuhara, H., Kobayashi, Y., Kaifu, N., Nagata, T., Gatley, I., Geballe, T. R. 1990, ApJ, 351, 89
- Pallavicini, R., Golub, L., Rosner, R., Vaiana, G. S., Ayres, T., Linsky, J. L. 1981, ApJ, 248, 279
- Parker, J. W. 1993, AJ, 106, 560
- Pollock, A. M. T. 1987, ApJ, 320, 283
- Portegies Zwart, S.F., Makino, J., McMillan, S.L.W. & Hut, P., 1999, A&A 348, 117,
- Prilutskii, O.F., Usov, V.V., 1976, Sov. Astr. 20, 2
- Puls, J., Kudritzki, R. ., Herrero, A., Pauldrach, A. W. A., Haser, S. M., Lennon, D. J., Gabler, R., Voels, S. A., Vilchez, J. M., Wachter, S., Feldmeier, A. 1996, A&A, 305, 171
- Schaerer, D., Maeder, A. 1992, A&A, 263, 129
- Sirianni, M., Nota, A., Leitherer, C., De Marchi, G., Clampin, M. 2000, ApJ, 533, 203

- Stevens, I., R., Blondin, J.M., Pollock, A.M.T., 1992, ApJ 386, 265
- Tanaka, Y., Lewin, W.H.G. 1995, X-ray binaries (eds. W.H.G.Lewin, J.A. van Paradijs & E.P.J. van den Heuvel), Cambridge Univ. Press, p.126
- Usov, V.V., 1992, ApJ 389, 635
- Vacca, W. D., Garmany, C. D., Shull, J. M. 1996, ApJ, 460, 914
- Walborn, N. R. 1973, ApJ, 182, L21
- Wang, Q., Helfand, D. J. 1991, ApJ, 370, 541
- Wang, Q. D., 1995, ApJ, 453, 783
- Weigelt, G., Baier, G. 1985, A&A, 150, L18
- Westerlund, B.E., 1960, Ark. Astron. 2, 419
- Westerlund, B.E., 1961, PASP 73, 61
- White, R. L., Long, K. S. 1986, ApJ, 310, 832